Analysis of the Wet-end Dynamics in Paper Mills

Jae Yong Ryu[1]· Yeong Koo Yeo[1] · Dong Jun Seo[2]· Hong Kang[3]

1) Department of Chemical Engineering, Hanyang University

2) Hansol Paper co., Ltd., · 3) J. J. Consulting

ABSTRACT

The wet-end dynamics of a paper mill was analyzed to characterize its dynamic behavior during the grade change. The model representing the wet-end section is developed based on the mass balance relationships written for the simplified wet-end white water network. From the linearization of the dynamic model, higher-order Laplace transfer functions were obtained followed by the reduction procedure to give simple lower-order models in the form of 1^{st}-order or 2^{nd}-order plus dead times. The dynamic response of the wet-end is influenced both by the white water volume and by the level of wire retention. Effects of key manipulated variables such as the thick stock flow rate, the ash flow rate and the retention aid flow rate on the major controlled variables were analyzed by numerical simulations. The simple dynamic model developed in the present study can be effectively used in the operation and control.

1. Introduction

The formation of a sheet of paper is a continuous process in which cellulose fibers, fines, fillers and additives form a network that is then pressed and dried. The three-dimensional network is formed by the mechanical entanglement of the fibers and by the chemical interactions between the different pulp fractions. The

complexity of the wet-end system of a paper mill is not readily apparent. The increased stringent environmental demands on paper production have led to the use of more closed wet-end systems with considerable material recirculation. It is possible to operate a paper machine successfully without a detailed understanding of how the changes in one part of the system will affect the other parts of the system. But, when operational troubles arise, it is necessary to interpret plant data correctly and to make cross check to the normal operating conditions of the plant. It is helpful to have current information on a particular system at hand when required, rather than to rely on spot sampled data with relatively low reliability. A dynamic model can be a powerful tool to provide reliable data for a particular section being considered. Apart from the process control and trouble-shooting for the wet-end section, the dynamic model can be an essential tool in the design of new systems and in the modification of existing systems [1], as well as in the analysis of process variables and in the identification of the effect of various additives on the dynamic behavior of the system.

Simple white water material balances for the wet-end system were proposed to compute equilibrium concentrations of solid components.[2] A steady-state model of this kind can be used to check the abnormality of the present operational status. With rapid development and application of various computer operation-aid systems, the operation of the plant is monitored and controlled on-line and the steady-state model can find its use only in very restricted area. Investigations on dynamics of the short circulation system with constant retentions were reported.[3] During the operation, retention changes due to machine speed changes, basis weight changes and retention aid changes. Retention changes have great effect on basis weight and ash percentage controls. However, there is no physically based dynamic model to predict the behavior of key controlled variables for given operating conditions. Dynamic model is especially useful to investigate the dynamic behavior of the wet-end system during the grade change. Use of a simple plant-wide dynamic model in the transition control during a grade

change was proposed.[4-6] Application of model predictive control schemes based on the transfer function dynamic models was also reported.[7]

The objective of the present work is to develop a simple dynamic model for a wet-end section to analyze the transient behavior of the white water network during the grade change. From the linearization of the dynamic model Laplace transfer functions representing the effects of key variables were developed. This kind of model for the paper mill was reported before.[8] The high-order (normally more than 4^{th} or 5^{th} order) transfer functions initially obtained from the linearization are not adequate in the model predictive control operations.[9] There are many benefits of simplified dynamic models such as less computational time, easier analysis and interpretation and convenient controller design. The model gives the bone-dry weight of the paper and dynamics of the retention for specific grade change operating conditions.

2. Materials & Methods

2.1 Simple short circulation

Fig. 1 shows the simplified wet-end system of a paper plant. In Fig. 1, the thick stock rate Q_0, the ash flow rate Q_f, the ash fraction of the thick stock X0a and the flow rate of the retention aid Q_p are assumed to be known, i.e., they are manipulated variables. These variables become input data for the model to be developed.

First we define a parameter p1 as

$$p1 = k \times Pw \times Sw \times Jr \times CF \times 1000 \quad [1]$$

k : draw factor, -

Pw : width of the pond, m

Sw : the gap of the slice, m

Jr : jet/wire ratio, -

CF : headbox slice factor, −

CF is the headbox slice factor which is dependent upon the configuration of the outlet device of the headbox. The product **Pw×Sw×CF** gives the area of the headbox outlet section. Jr is defined as the ratio of the flow rate from the headbox to the wire speed. In normal operations, Jr is slightly greater than 1. Due to the draw in the drying section, the paper web moves faster in the reel section than in the wire. The factor **k** represents the difference in the speed between the wire section and the reel part. In most operations the speed in the wire section is 97% of the speed in the reel section. This means that we can set the value of **k** as 0.97 in most cases. The flow rate from the headbox Q_s is given by

$$Q_s = \mathrm{p1} \cdot V_r$$

[2]

Q_s : outlet flow rate from the headbox, L/min

V_r : reel speed, m/min

where Q_s is the jet flow rate form the slice taking into account of the effect of Vena contractor. The flow rate to the press is then expressed as

$$Q_d = \frac{\mathrm{p1} \cdot Vr \cdot C_s \cdot R}{C_d} \qquad [3]$$

C_s : consistency in the headbox, kg/L or %/100

R : retention ratio, −

C_d : consistency to press, kg/L or %/100

where C_d lies in the range of 18 22% and is set to 20% in the simulations. The product $\mathrm{p1} \cdot Vr \cdot C_s$ is the amount of the mass from the headbox. From the simple material balance around the wire and the tray, the flow rate Q_T of the stream to the silo and the seal pit is given by

$$Q_T = Q_s - Q_d = \mathrm{p1} \cdot V_r - \frac{\mathrm{p1} \cdot V_r \cdot C_s \cdot R}{C_d}$$

[4]

Q_T : flow rate in the tray, L/min

Q_d : flow rate to the press, L/min

The flow rate of the stream to save-all Q_{pdf} can be obtained from the material balance around the wire, the silo and the seal pit and can be expressed as

$$Q_{pdf} = \mathrm{p1} \cdot V_r - \mathrm{p2} \cdot V_r \cdot C_s \cdot R + \mathrm{Vw1} - (\mathrm{p1} \cdot V_r - Q_0 - Q_f - Q_p - \mathrm{Vw})$$

[5]

Q_{pdf} : flow rate to saveall, L/min

Q_0 : thick stock flow rate, L/min

Q_f : ash flow rate, L/min

Q_p : flow rate of the retention aid, L/min

Vw : the amount of dilution water, L/min

Vw1 : clean water rate to the silo, L/min

where p2 is given by

$\mathrm{p2} = \mathrm{p1}/C_d$

Q_2 is the flow rate of the internal circulation stream and is given by

$$Q_2 = \mathrm{p1} \cdot V_r - Q_0 - Q_f - Q_p - \mathrm{Vw} \qquad [6]$$

Q_2 : internal recirculation flow rate, L/min

Perfect mixing in all the components (Fig.1) with significant volume is assumed in this simplified model.

2.2 Silo and Stock approach section

Dynamics of the solid and ash contents in the silo and the seal pit can be expressed as

$$\frac{dC_2}{dt} = \left((1-R)\cdot \mathrm{p1}\cdot V_r \cdot C_s - Q_2 \cdot C_2 + (\mathrm{p1}\cdot V_r - \mathrm{p2}\cdot V_r \cdot C_s \cdot R + \mathrm{Vw1} - Q_2)\cdot C_2\right)/\mathrm{V} \quad [7]$$

C_2 : consistency in the silo, kg/L or %/100

V : silo and sealpit volume, L^3

$$\frac{dX_{2a}}{dt} = \left(\begin{array}{l}(1-R_a)\cdot \mathrm{p1}\cdot V_r \cdot C_s \cdot X_{sa} - Q_2 \cdot C_2 \cdot X_{2a} - \ldots \\ \left(\mathrm{p1}\cdot V_r - \mathrm{p2}\cdot V_r \cdot C_s \cdot R + \mathrm{Vw1} - Q_2\right)\cdot C_2 \cdot X_{2a}\end{array}\right)/\mathrm{V}/C_2 - \frac{X_{2a}}{C_2}\frac{dC_2}{dt} \quad [8]$$

R_a : ash retention ratio, –

X_{2a} : ash fraction in the silo, –

X_{sa} : ash fraction in the headbox, –

Similarly, dynamics in the stock approach section are given by

$$\frac{dC_s}{dt} = \left(Q_0 C_s + (\mathrm{p1}\cdot V_r - Q_0 - Q_f - Q_p - \mathrm{Vw})\cdot C_2 + Q_f \cdot C_f - \mathrm{p1}\cdot V_r \cdot C_s\right)/\mathrm{Vs} \quad [9]$$

Vs : stock approach volume, L^3

C_f : consistency in the filler flow, kg/L or %/100

$$\frac{dX_{sa}}{dt} = \left(Q_0 \cdot C_0 \cdot X_{0a} + (\mathrm{p1}\cdot V_r - Q_0 - Q_f - Q_p - \mathrm{Vw})\cdot C_2 \cdot X_{2a} + Q_f \cdot C_f - \mathrm{p1}\cdot Vr \cdot Cs \cdot X_{sa}\right)/\mathrm{Vs}/C_s - \ldots$$

$$\frac{X_{sa}}{C_s}\left(Q_0 \cdot C_s + (\mathrm{p1}\cdot V_r - Q_0 - Q_f - Q_p - \mathrm{Vw})\cdot C_2 + Q_f \cdot C_f - \mathrm{p1}\cdot V_r \cdot C_s\right)/\mathrm{Vs} \quad [10]$$

X_{0a} : ash fraction in the thick stock, –

C_0 : consistency in the thick stock, kg/L or %/100

In this study, the stock approach section includes screens and cleaners as well as deculator. Because of the complexity of the configuration of cleaner sections and screens and of the considerable volume of the deculator, we supposed a tank with volume Vs to represent the stock approach section. We assumed that the flow from the tank becomes the outlet flow from the headbox. Vs includes the volume of the deculator, the volume of the 1st and 2nd cleaner lines and the volume of 1st and 2nd screen lines.

2.3 Retention and BD

Retention is affected by many factors such as the amount and types of retention aids, thick stock rates, types of pulp, SRE (specific refinery energy), fiber fine fraction in the thick stock, the wire speed, filler flow rates, temperature of the white water, PH, ash contents in the white water and the thick stock, and the wire mesh. [10] In this work we are considering only the "short-term dynamics" during grade changes rather than the "long-term dynamics" . Then we can assume that retentions exhibit the first-order dynamics and can represent the behavior of R and R_a as

$$\frac{dR}{dt} = \frac{k1}{\tau} Q_p - \frac{R}{\tau} \qquad [11]$$

k1 : retention constant, min/L

$$\frac{dR_a}{dt} = \frac{k2}{\tau} Q_p - \frac{R_a}{\tau} \qquad [12]$$

k2 : ash retention constant, min/L

τ : retention time constant, min

k2 was assumed to be 1/3 of k1. k1 can be obtained from the steady-state retention and the amount of the retention aid. τ depends on the specific paper machine being used.

The bone dry weight *BD* and the ash bone dry *ashBD* are given by

$$BD = \mathrm{p1} \times \mathrm{p3} \times C_s \times R \quad [13]$$

BD : bone-dry basis weight, g/m^2

$$ashBD = \mathrm{p1} \times \mathrm{p3} \times C_s \times X_{sa} \times R_a \quad [14]$$

ashBD : bone-dry basis weight of ash, g/m^2

$$\mathrm{p3} = \frac{\mathrm{Cw} \times \mathrm{Wr} \times 1000}{\mathrm{Pw} \times \mathrm{Rw}} \quad [15]$$

Cw : the width of the couch, m

Rw : the width of the reel, m

Wr : diminishment ratio, -

where Wr is the diminishment ratio of BD or ash BD which can be occurred unexpectedly while the paper web passes the press and dryer section.

2.4 State-space model

The reel speed, the thick stock flow, the filler flow, the retention aid flow, and the ash fraction of the thick stock serve as input variables in the model presented before (Eqs. [1]~[15]). The thick stock flow and the ash fraction affect BD and ashBD is not influenced by these variables. The state variables are C_2, C_s, X_{2a}, X_{sa}, R and R_a. The two outputs are BD (bone dry weight) and ashBD (bone dry ash weight). The ash fraction of the thick stock was assumed to follow a ramp trajectory during the grade change operation. The linearized state equations are given by

$$\dot{X} = AX + BU \quad [16]$$
$$Y = CX + DU$$

where

$$X = \left[C_2 \;\; X_{2a} \; C_s \; X_{sa} \; R \; R_a \;\right]'$$

$$U = \left[Vr \; Q_0 \; Q_f \; Q_p \; X_{0a} \right]'$$

$$Y = \left[BD \; ashBD \right]'$$

Elements of the state-space system [16] are given by

$$\begin{pmatrix} C_2' \\ X_{2a}' \\ C_s' \\ X_{sa}' \\ R' \\ R_a' \end{pmatrix} = \begin{pmatrix} \frac{\partial C_2}{\partial C_2}\Big|_s & \frac{\partial C_2}{\partial X_{2a}}\Big|_s & \frac{\partial C_2}{\partial Cs}\Big|_s & \frac{\partial C_2}{\partial X_{sa}}\Big|_s & \frac{\partial C_2}{\partial R}\Big|_s & \frac{\partial C_2}{\partial R_a}\Big|_s \\ \frac{\partial X_{2a}}{\partial C_2}\Big|_s & \frac{\partial X_{2a}}{\partial X_{2a}}\Big|_s & \frac{\partial X_{2a}}{\partial Cs}\Big|_s & \frac{\partial X_{2a}}{\partial X_{sa}}\Big|_s & \frac{\partial X_{2a}}{\partial R}\Big|_s & \frac{\partial X_{2a}}{\partial R_a}\Big|_s \\ \frac{\partial C_s}{\partial C_2}\Big|_s & \frac{\partial C_s}{\partial X_{2a}}\Big|_s & \frac{\partial C_s}{\partial Cs}\Big|_s & \frac{\partial C_s}{\partial X_{sa}}\Big|_s & \frac{\partial C_s}{\partial R}\Big|_s & \frac{\partial C_s}{\partial R_a}\Big|_s \\ \frac{\partial X_{sa}}{\partial C_2}\Big|_s & \frac{\partial X_{sa}}{\partial X_{2a}}\Big|_s & \frac{\partial X_{sa}}{\partial Cs}\Big|_s & \frac{\partial X_{sa}}{\partial X_{sa}}\Big|_s & \frac{\partial X_{sa}}{\partial R}\Big|_s & \frac{\partial X_{sa}}{\partial R_a}\Big|_s \\ \frac{\partial R}{\partial C_2}\Big|_s & \frac{\partial R}{\partial X_{2a}}\Big|_s & \frac{\partial R}{\partial Cs}\Big|_s & \frac{\partial R}{\partial X_{sa}}\Big|_s & \frac{\partial R}{\partial R}\Big|_s & \frac{\partial R}{\partial R_a}\Big|_s \\ \frac{\partial R_a}{\partial C_2}\Big|_s & \frac{\partial R_a}{\partial X_{2a}}\Big|_s & \frac{\partial R_a}{\partial Cs}\Big|_s & \frac{\partial R_a}{\partial X_{sa}}\Big|_s & \frac{\partial R_a}{\partial R}\Big|_s & \frac{\partial R_a}{\partial R_a}\Big|_s \end{pmatrix} \begin{pmatrix} C_2' \\ X_{2a}' \\ C_s' \\ X_{sa}' \\ R' \\ R_a' \end{pmatrix} + \begin{pmatrix} \frac{\partial C_2}{\partial V_r}\Big|_s & \frac{\partial C_2}{\partial Q_0}\Big|_s & \frac{\partial C_2}{\partial Q_f}\Big|_s & \frac{\partial C_2}{\partial Q_p}\Big|_s & \frac{\partial C_2}{\partial X_{0a}}\Big|_s \\ \frac{\partial X_{2a}}{\partial V_r}\Big|_s & \frac{\partial X_{2a}}{\partial Q_0}\Big|_s & \frac{\partial X_{2a}}{\partial Q_f}\Big|_s & \frac{\partial X_{2a}}{\partial Q_p}\Big|_s & \frac{\partial X_{2a}}{\partial X_{0a}}\Big|_s \\ \frac{\partial C_s}{\partial V_r}\Big|_s & \frac{\partial C_s}{\partial Q_0}\Big|_s & \frac{\partial C_s}{\partial Q_f}\Big|_s & \frac{\partial C_s}{\partial Q_p}\Big|_s & \frac{\partial C_s}{\partial X_{0a}}\Big|_s \\ \frac{\partial X_{sa}}{\partial V_r}\Big|_s & \frac{\partial X_{sa}}{\partial Q_0}\Big|_s & \frac{\partial X_{sa}}{\partial Q_f}\Big|_s & \frac{\partial X_{sa}}{\partial Q_p}\Big|_s & \frac{\partial X_{sa}}{\partial X_{0a}}\Big|_s \\ \frac{\partial R}{\partial V_r}\Big|_s & \frac{\partial R}{\partial Q_0}\Big|_s & \frac{\partial R}{\partial Q_f}\Big|_s & \frac{\partial R}{\partial Q_p}\Big|_s & \frac{\partial R}{\partial X_{0a}}\Big|_s \\ \frac{\partial R_a}{\partial V_r}\Big|_s & \frac{\partial R_a}{\partial Q_0}\Big|_s & \frac{\partial R_a}{\partial Q_f}\Big|_s & \frac{\partial R_a}{\partial Q_p}\Big|_s & \frac{\partial R_a}{\partial X_{0a}}\Big|_s \end{pmatrix} \begin{pmatrix} V_{reel}' \\ Q_0' \\ Q_f' \\ Q_p' \\ X_{0a}' \end{pmatrix}$$

$$\begin{pmatrix} BD' \\ ashBD' \end{pmatrix} = \begin{pmatrix} \frac{\partial BD}{\partial C_2}\Big|_s & \frac{\partial BD}{\partial X_{2a}}\Big|_s & \frac{\partial BD}{\partial Cs}\Big|_s & \frac{\partial BD}{\partial X_{sa}}\Big|_s & \frac{\partial BD}{\partial R}\Big|_s & \frac{\partial BD}{\partial R_a}\Big|_s \\ \frac{\partial aB}{\partial C_2}\Big|_s & \frac{\partial aB}{\partial X_{2a}}\Big|_s & \frac{\partial aB}{\partial Cs}\Big|_s & \frac{\partial aB}{\partial X_{sa}}\Big|_s & \frac{\partial aB}{\partial R}\Big|_s & \frac{\partial aB}{\partial R_a}\Big|_s \end{pmatrix} \begin{pmatrix} C_2' \\ X_{2a}' \\ C_s' \\ X_{sa}' \\ R' \\ R_a' \end{pmatrix} + \begin{pmatrix} \frac{\partial BD}{\partial V_r}\Big|_s & \frac{\partial BD}{\partial Q_0}\Big|_s & \frac{\partial BD}{\partial Q_f}\Big|_s & \frac{\partial BD}{\partial Q_p}\Big|_s & \frac{\partial BD}{\partial X_{0a}}\Big|_s \\ \frac{\partial aB}{\partial V_r}\Big|_s & \frac{\partial aB}{\partial Q_0}\Big|_s & \frac{\partial aB}{\partial Q_f}\Big|_s & \frac{\partial aB}{\partial Q_p}\Big|_s & \frac{\partial aB}{\partial X_{0a}}\Big|_s \end{pmatrix} \begin{pmatrix} V_r' \\ Q_0' \\ Q_f' \\ Q_p' \\ X_{0a}' \end{pmatrix}$$

The elements of the coefficient matrices in the above relations can be evaluated from Esq. [7]~[14]. Resulting state equations can be expressed as

$$\begin{pmatrix} C_2' \\ X_{2a}' \\ C_s' \\ X_{sa}' \\ R' \\ R_a' \end{pmatrix} = \begin{pmatrix} A_{11} & A_{12} & A_{13} & A_{14} & A_{15} & A_{16} \\ A_{21} & A_{22} & A_{23} & A_{24} & A_{25} & A_{26} \\ A_{31} & A_{32} & A_{33} & A_{34} & A_{35} & A_{36} \\ A_{41} & A_{42} & A_{43} & A_{44} & A_{45} & A_{46} \\ A_{51} & A_{52} & A_{53} & A_{54} & A_{55} & A_{56} \\ A_{61} & A_{62} & A_{63} & A_{64} & A_{65} & A_{66} \end{pmatrix} \begin{pmatrix} C_2' \\ X_{2a}' \\ C_s' \\ X_{sa}' \\ R' \\ R_a' \end{pmatrix} + \begin{pmatrix} B_{11} & B_{12} & B_{13} & B_{14} & B_{15} \\ B_{21} & B_{22} & B_{23} & B_{24} & B_{25} \\ B_{31} & B_{32} & B_{33} & B_{34} & B_{35} \\ B_{41} & B_{42} & B_{43} & B_{44} & B_{45} \\ B_{51} & B_{52} & B_{53} & B_{54} & B_{55} \\ B_{61} & B_{62} & B_{63} & B_{64} & B_{65} \end{pmatrix} \begin{pmatrix} V_{reel}' \\ Q_0' \\ Q_f' \\ Q_p' \\ X_{0a}' \end{pmatrix} \quad [17]$$

$$Y = CX + DU$$

In eq. [17], the subscript s denotes the steady-state values.

2.5 Higher-order transfer functions

Initial higher-order Laplace transfer functions can be expressed in the form as given by

$$\begin{pmatrix} BD' \\ ashBD' \end{pmatrix} = \begin{pmatrix} G_{11}(s) & G_{12}(s) & G_{13}(s) & G_{14}(s) & G_{15}(s) \\ G_{21}(s) & G_{22}(s) & G_{23}(s) & G_{24}(s) & G_{25}(s) \end{pmatrix} \begin{pmatrix} V_r' \\ Q_0' \\ Q_f' \\ Q_p' \\ X_{0a}' \end{pmatrix}$$

[18]

where

$$G_{11} = \frac{-0.05514\ s - 0.02449}{s^2 + 1.849\ s + 0.4314}$$

[19]

$$G_{21} = \frac{-0.00584\ s^3 - 0.01532\ s^2 - 0.01113\ s - 0.003428}{s^4 + 4.035\ s^3 + 5.208\ s^2 + 2.303\ s + 0.3172}$$

[20]

$$G_{12} = \frac{0.005123\,s + 0.002654}{s^2 + 1.849\,s + 0.4314}$$

[21]

$$G_{22} = \frac{0.0001507\,s^3 + 0.0003805\,s^2 + 0.0003251\,s + 0.000251}{s^4 + 4.035\,s^3 + 5.208\,s^2 + 2.303\,s + 0.3172}$$

[22]

$$G_{13} = \frac{0.07596\,s + 0.03448}{s^2 + 1.849\,s + 0.4314}$$

[23]

$$G_{23} = \frac{0.03988\,s^3 + 0.11\,s^2 + 0.08459\,s + 0.01779}{s^4 + 4.035\,s^3 + 5.208\,s^2 + 2.303\,s + 0.3172}$$

[24]

$$G_{14} = \frac{0.008795\,s^2 + 0.01705\,s - 0.001384}{s^3 + 1.856\,s^2 + 0.4437\,s + 0.002876}$$

[25]

$$G_{24} = \frac{0.0006863\,s^5 + 0.0029\,s^4 + 0.003684\,s^3 + 0.0006853\,s^2 - 0.0008424\,s - 5.645e\text{-}006}{s^6 + 4.048\,s^5 + 5.262\,s^4 + 2.372\,s^3 + 0.3482\,s^2 + 0.004332\,s + 1.41e\text{-}005}$$

[26]

$$G_{15} = 0$$

[27]

$$G_{25} = \frac{29.29\,s + 26.99}{s^2 + 2.186\,s + 0.7353}$$

[28]

Pole-zero locations of these functions are shown in Fig 2. There are no poles with positive real values and we can confirm that the wet-end system is stable. But $G_{14}(s)$ and $G_{24}(s)$ gives positive zeros, which means that inverse responses are expected in BD and ashBD due to the change in the retention aid flow.

2.6 Reduction of the transfer functions

Higher-order transfer functions may cause numerical errors and increase computational load when they are used in the simulations or in the control operations such as the model predictive control. In fact, it is very difficult to formulate model predictive control problems by using higher-order transfer functions. Most chemical plants can be expressed by the transfer functions in the form of 1^{st}-order plus dead time (FOPDT) or 2^{nd}-order plus dead time (SOPDT). SOPDT is used to relate the input and the output characterized by inverse responses. In the identification of lower-order models, we first assume FOPDT or SOPDT models with unknown parameters. The higher-order model (18) serves as the actual plant. A simple pulse input as shown in Fig. 3 is introduced into the supposed models and the "plant" simultaneously and compare the resulting outputs. Use of the PRBS (pseudo-random binary sequence) is the usual practice in this case. But a simple pulse function was found to be enough in the identification of the lower-order models. By minimization of the difference (29) between the supposed model output and the "plant" output, we can determine the best possible model parameters.

$$Q(F,Y)=\sum_{i=1}^{n}\left[F_i-Y_i\right]^2 \qquad [29]$$

F_i : F_i is the output from the higher-order model

Y_i : Y_i is the output computed from the assumed FOPDT or SOPDT model.

I : i is the sampling number

Various optimization algorithms can be used in the minimization but the simple least-squares method was enough for our purpose. Resulting lower-order transfer functions can be expressed as following:

$$\begin{pmatrix} Y1 \\ Y2 \end{pmatrix} = \begin{pmatrix} \frac{-0.05242 \cdot e^{-\theta_{11}}}{1.253s+1} & \frac{0.005675 \cdot e^{-\theta_{12}}}{1.572s+1} & \frac{0.07373 \cdot e^{-\theta_{13}}}{1.294s+1} & \frac{(0.1322s+0.009898) \cdot e^{-\theta_{14}}}{13.82s^2+4.198s+1} & \frac{-1e\text{-}09 \cdot e^{-\theta_{15}}}{10s+1} \\ \frac{-0.01008 \cdot e^{-\theta_{21}}}{3.427s+1} & \frac{0.001334 \cdot e^{-\theta_{22}}}{14.23s+1} & \frac{0.05274 \cdot e^{-\theta_{23}}}{1.92s+1} & \frac{(0.1322s+0.009898) \cdot e^{-\theta_{24}}}{13.82s^2+4.198s+1} & \frac{35.53 \cdot e^{-\theta_{25}}}{1.608s+1} \end{pmatrix} \begin{pmatrix} U1 \\ U2 \\ U3 \\ U4 \\ U5 \end{pmatrix}$$

[30]

θ_{ij} : dead times, min

Dead times can easily be determined by using operational data. It is almost impossible to obtain exact values for the dead times. Fig. 4 shows the steps to determine dead times. First, initial values of dead times θ_{ij} are assumed and iterative minimizations of residuals are followed to give optimal dead times. Results of dead time computations are given by (31).

$$\theta_{\min} = \begin{pmatrix} 0 & 1.3 & 0.3751 & 0.9865 & 1.3 \\ 0 & 1.3 & 0.3751 & 0.9865 & 1.3 \end{pmatrix}$$

[31]

3. Results & Discussion

Suitable initial values for the state variables C_s, X_{sa}, C_2, X_{2a}, R and R_a should be assigned for the computations to be possible. Usually steady-state values for these variables are used as initial values. Table 1 shows initial values for the state variables used in the present work. Data set obtained from the grade change operations were used to validate the simplified dynamic model. The first data set, being compared with the results of the simulation, was obtained during the change of the bone-dry weight (BD) from 66 g/m^2 to 56 g/m^2 (or from 70.8 g/m^2 to

61 g/m^2 in the basis weight (BW)).

In the model, rates of the thick stock flow, the retention aid and the filler inlet and the reel speed serve as input variables. Fig. 5 and 6 show changes of input variables used both in the actual plant operation and in the simulation. The ash fraction in the thick stock flow, X_{0a}, is dependent upon the extent of mixing of raw materials in the Broke and machine chest. X_{0a} exerts a strong influence on the ash content at the reel box, although BD is not affected by X_{0a}. The magnitude of X_{0a} is changed according to the paper grade. For this reason, the ash fraction should be considered as an input variable.[6, 11] The ash fraction in the thick stock flow was assumed to exhibit the 2nd-order characteristics as given by

$$Y(s) = G(s) \cdot \frac{\Delta X_{0a}}{s} \qquad G(s) = \frac{1}{\tau_a^2 s^2 + 2\xi\tau s + 1}$$

[32]

τ_a : 2nd order transfer function time constant, min

ζ : 2nd order transfer function damping

where τ_a=18 and ζ=1 in the present study.

The same input variables were fed into the plant as well as the model. Results of the simulations are shown in Figs. 7, 8 and 9. Two key output variables (BD and ash BD) and four major state variables (consistencies in the silo and the headbox, the slurry rate and the retention ratio) were computed. Even with the up-to-date DCS technology, not all the variables are measured in the operation. In the plant being considered, BD and ash BD were detected online. We can see that the simplified model developed in the present study exhibit satisfactory tracking performance to the plant. The computed consistencies in the silo and the headbox shown in Fig. 8 display dynamic characteristics as expected. The smooth behavior of the silo consistency is not surprising considering the assumption of perfect mixing in the silo. Fig. 9 shows the slurry rate and the retention ratio

obtained from the simulation. The retention ratio is another variable being detected online. The cause of the big discrepancy in the beginning is not clarified yet. But, without knowledge on the details of the detecting mechanism of the retention ratio, we can only say that the assumption of the perfect mixing in the silo might cause the discrepancy.

4. Conclusions

A dynamic model for the wet-end section of a paper mill was developed to characterize its dynamic behavior during the grade change. The model is based on the mass balance relationships written for the simplified wet-end white water network. From the linearization of the dynamic model followed by Laplace transformation, higher-order transfer function models were obtained and stability of the models was examined. The 1^{st}-order plus dead time (FOPDT) and 2^{nd}-order plus dead time (SOPDT) models were identified based on the higher-order models by using least-squares method. Effects of key manipulated variables such as the thick stock flow, the filler flow and the retention aid flow on the major controlled variables were analyzed by numerical simulations. Results of simulations show a little discrepancy from the operational data and we can see that the dynamics of the wet-end section of paper plants can be represented well by transfer functions with low-order plus dead times. The dynamic model developed in the present study in the form of Laplace transfer functions can be effectively used in the operation and control.

ACKNOWLEDGEMENT

The authors would like to thank Mr. Yeong-jun Lee at Hansol paper Co. for his

cooperation in providing information and data for this paper. This work was supported by Korea Institute of Industrial Technology and in part by the research fund of Hanyang University (HY-2002-T).

Literature Cited

1. Yeo, Y. K., Roh, H. D., Kim, I. W., Moon, I., And Chung, Y., Korean J. Chem. Eng., 20(2): 200 (2003).
2. Mardon, J., Jackson, M. and Serenius, R., Appita J, 25(1): 45(1971).
3. Norman, Bo., EUCEPA 1990 Print Paper and Board Products for Printing in the Nineties Conference Proceedings, EUCEPA, Paris, p. 217
4. Murphy, T. F., and Chen, S. C., Proceedings of the 1999 IEEE international conference on control Applications, IEEE, Hawaii, p. 1278.
5. Skoglund, A., and Brundin, A., Nordic Pulp and Paper Res J., 15(3): 183(2000).
6. Vhtamaki, P., Pulp Paper Can, 102(7): 30(2001).
7. Hauge, T. A., and Lie, B., Modeling, Identification and Control, 23(1): 27(2002).
8. Berrada, M. E., Tarasiewicz, S., Elkadiri, M. E., and Radziszewski, P. H., IEEE Transactions on Industrial Electronics, 44(4): 579(1997).
9. Chyi, H. and Chuang, Y., Chem. Eng..Sci, 49(19): 3291(1994).
10. Neimo, L., Papermaking Science and Technology: Paper making chemistry (Book 4), Ch. 4, Tappi press, Helsinki, (2000)
11. Elkadiri, M. E., and Berrada, M. E., Conference Record of 1997 Annual Pulp and Paper Industry Technical Conference, IEEE, Cincinnati. OH, p. 97.

Table 1. Initial values for state variables

State variables	C_s (kg/l or %/100)	X_{sa} (−)	C_2 (kg/l or %/100)	X_{2a} (−)	R (%)	R_a (%)
	0.009	0.235	0.0022	0.47	75	51

Table 2. Constants and parameters

Description	
C_0 (kg/L) or (%/100)	0.0328
C_f (kg/L) or (%/100)	0.47
C_d (kg/L) or (%/100)	0.2
V (Liter)	105,000
Vs (Liter)	50,000
Vw (Liter)	1,000
Vw1 (Liter)	2,000
k1 (min/L)	0.0142
τ (min)	800
Pw (Meter)	5.65
Rw (Meter)	4.06
Cw (Meter)	5.17
Sw (Meter)	0.01021
CF (−)	0.92
Jr (−)	1.04
Wr (−)	0.85

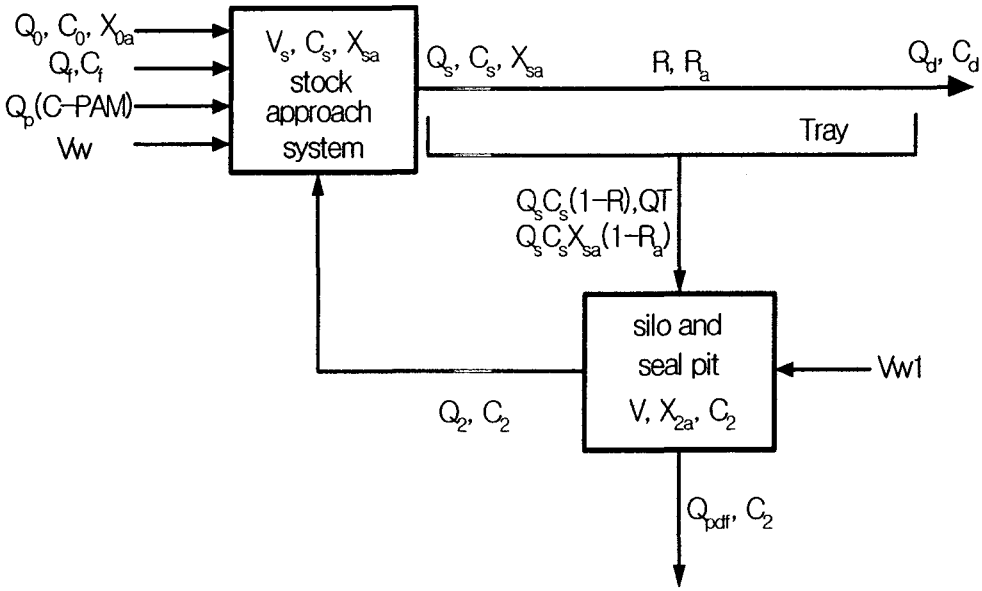

Figure 1. Schematics of wet-end ystem

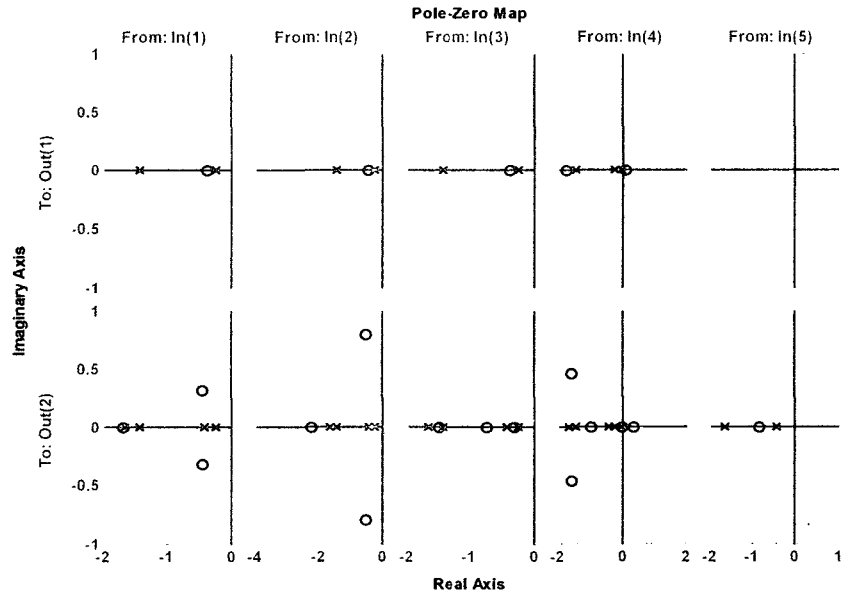

Figure 2. Pole-zero map (x: pole, o: zero).

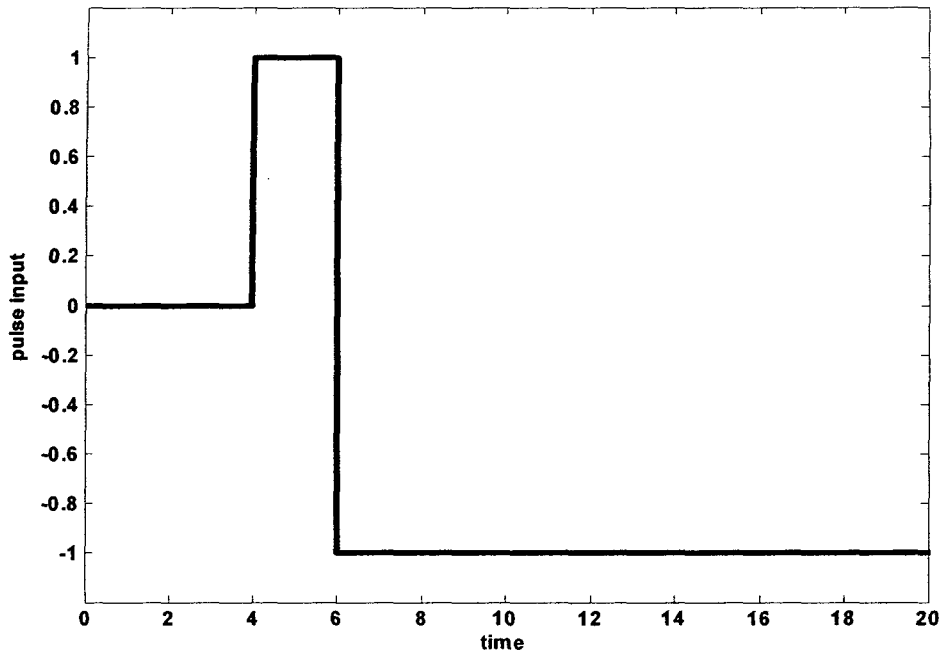

Figure 3. Pulse input used in the identification of lower-order models.

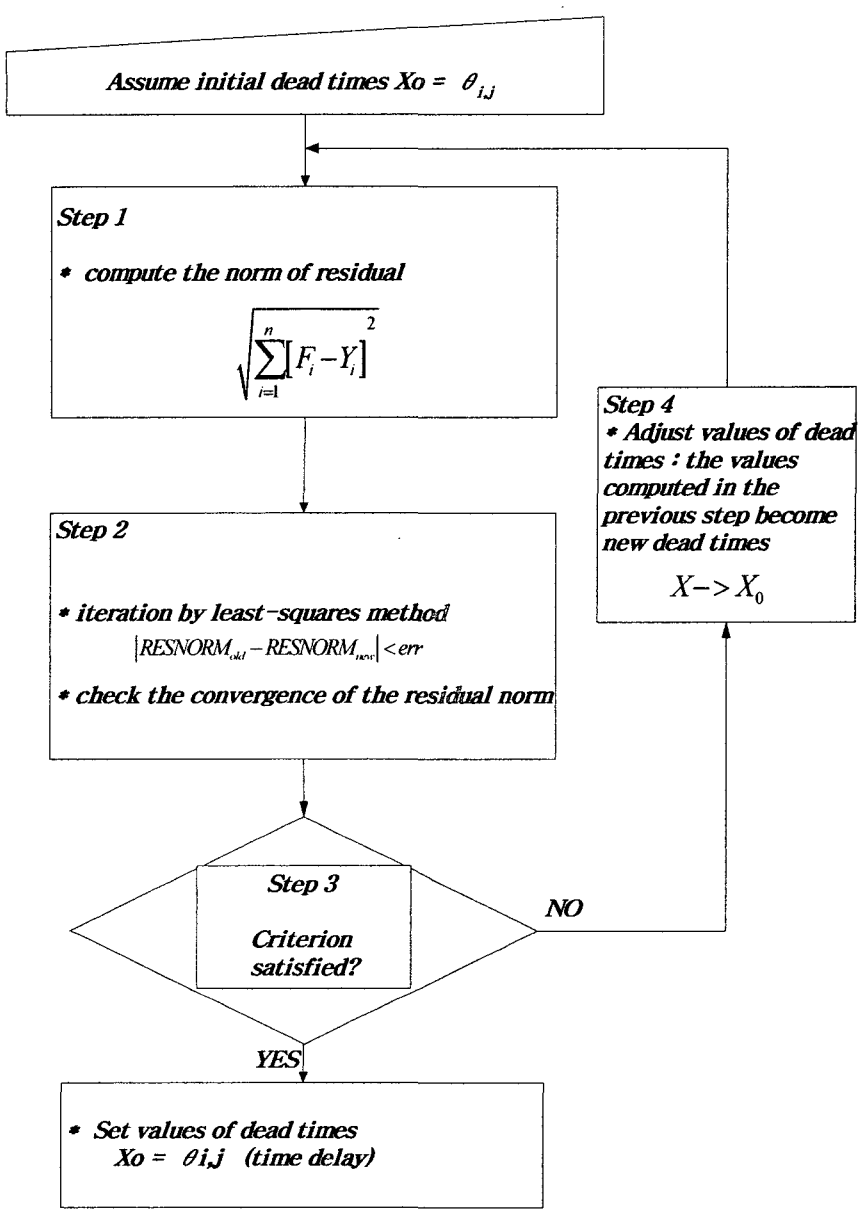

Figure 4. Procedure for the determination of dead times.

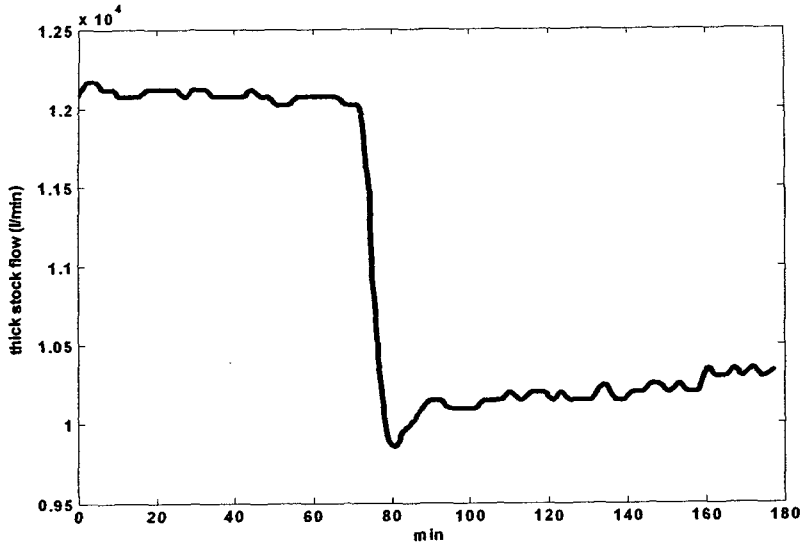

(a)

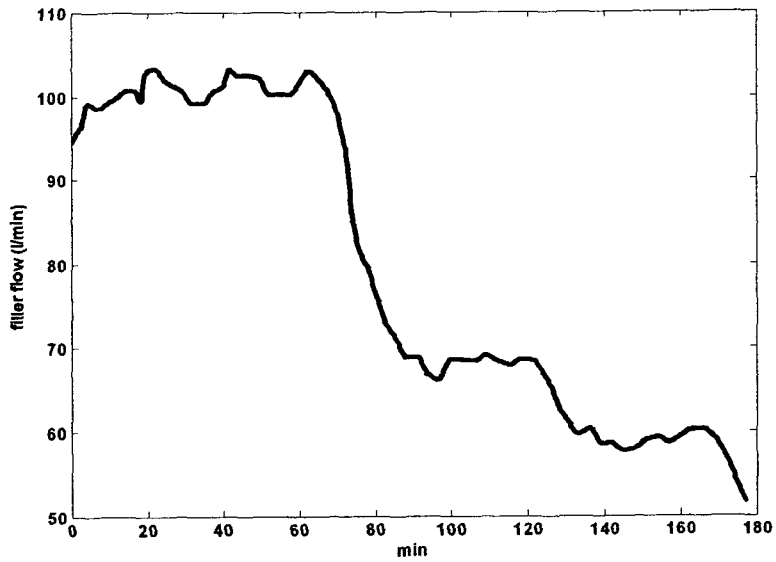

(b)

Figure 5. Input flow rates of stock (a) and filler (b)

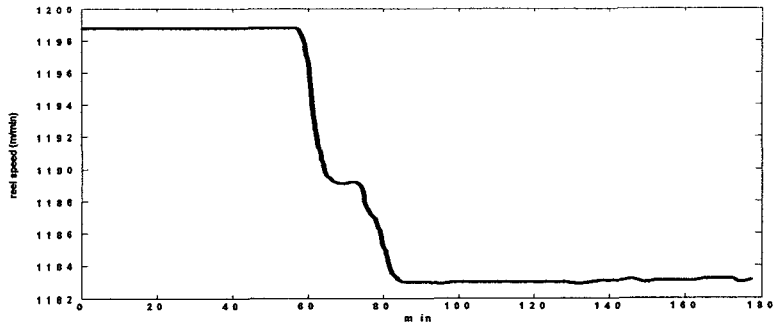

(a)

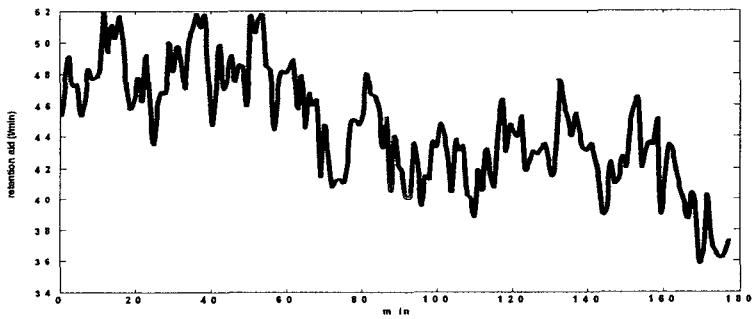

(b)

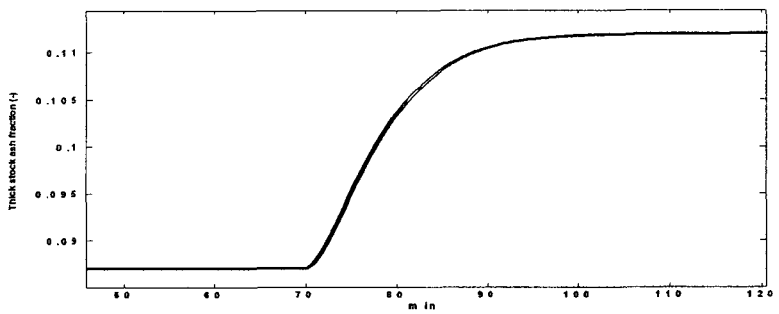

(c)

Figure 6. Reel speed (a), flow rates of the retention aid (b), thick stock ash fraction (c)

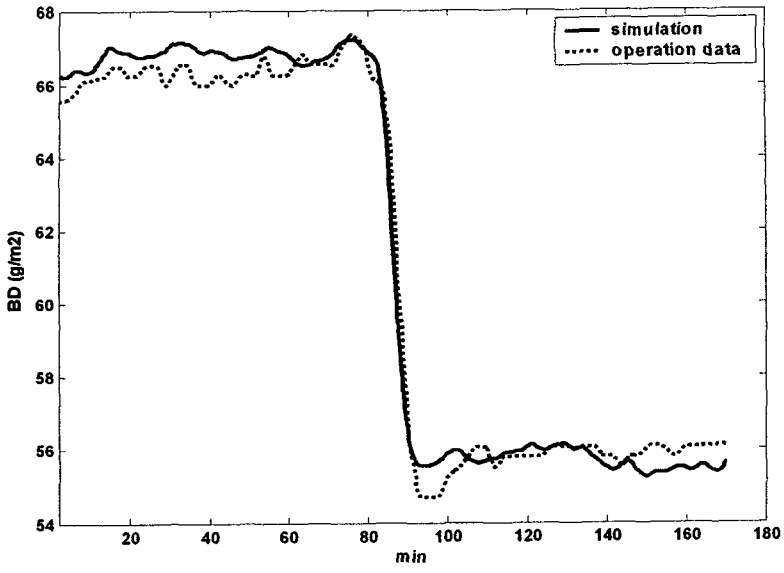

(a)

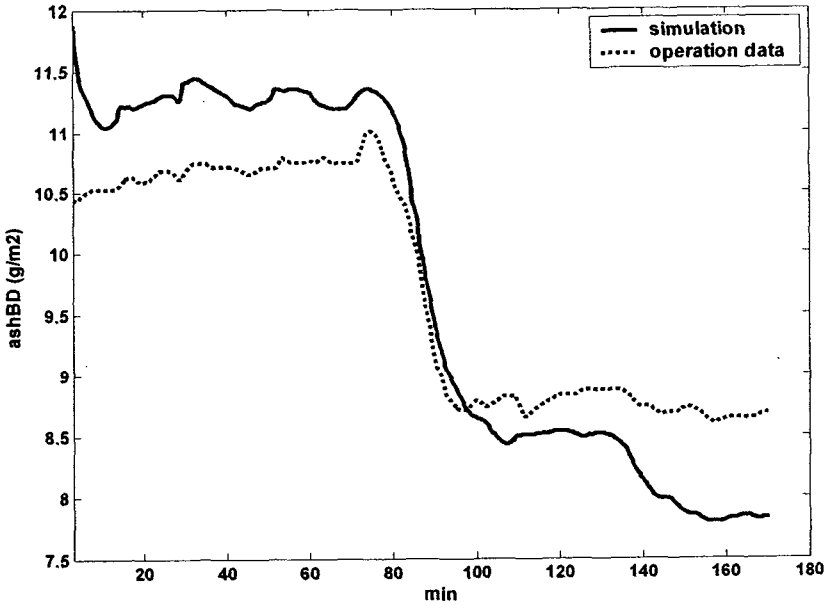

(b)

Figure 7. Dynamics of bone-dry weight (a) and ash bone-dry weight (b)

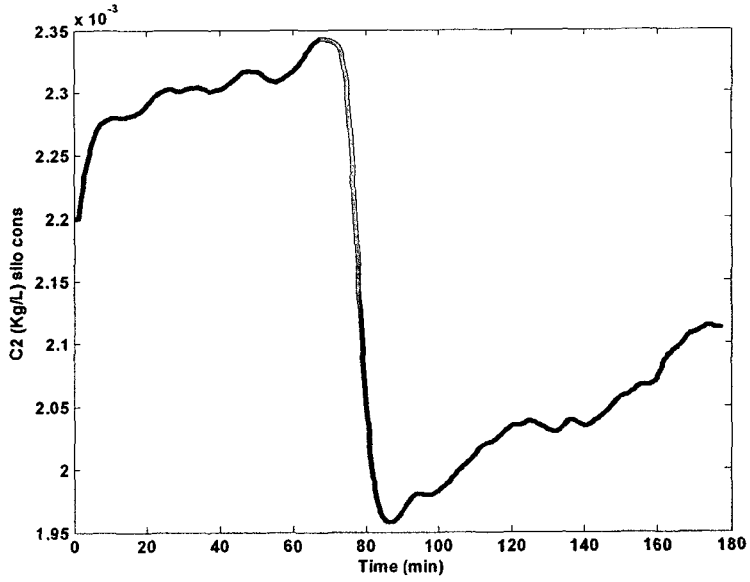

(a)

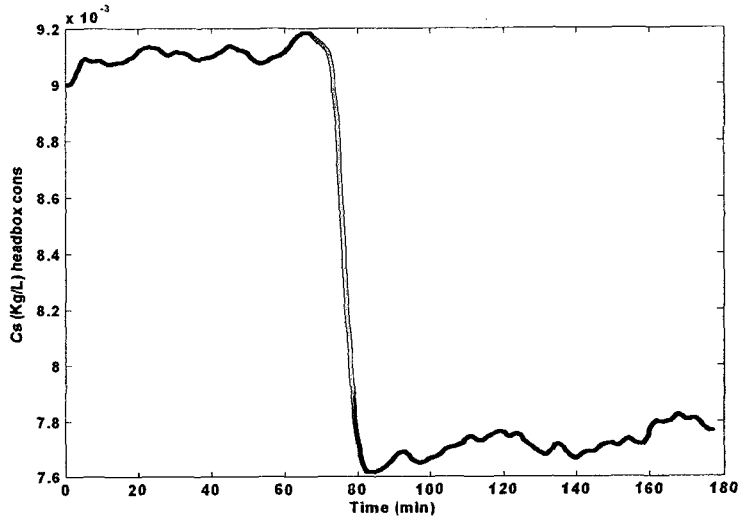

(b)

Figure 8. Dynamics of silo consistency (a) and headbox consistency (b)

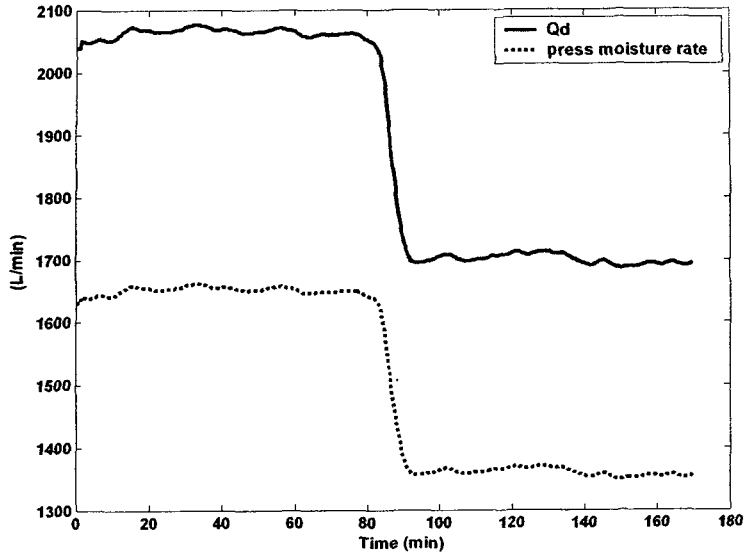

(a)

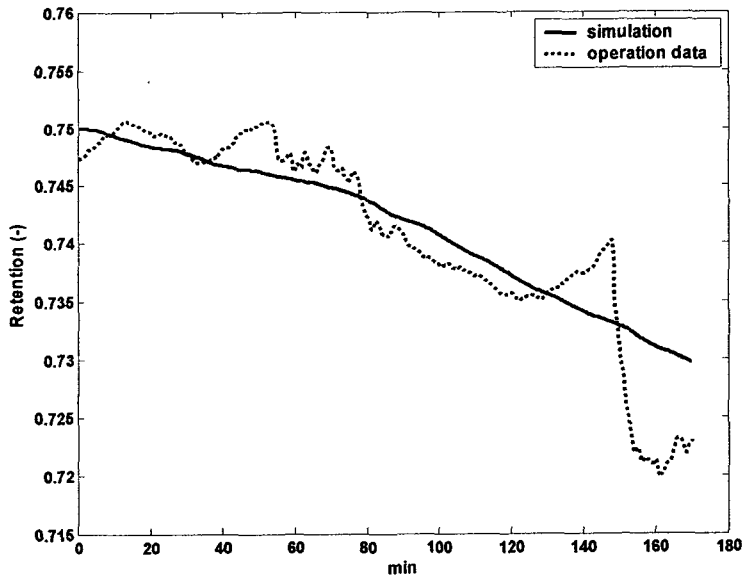

(b)

Figure 9. Dynamics of slurry and moisture rates to the press (a) and retention ratio (b)